MINDLN 부채꼴형 평판의 진동해석

VIBRATION ANALYSIS OF MINDLIN SECTORIAL PLATES

김 주 우* 한 봉 구**
Kim, Joo-Woo Han, Bong-Koo

ABSTRACT

This paper provides accurate flexural vibration solutions for thick (Mindlin) sectorial plates. A Ritz method is employed which incorporates a complete set of admissible algebraic-trigonometric polynomials in conjunction with an admissible set of Mindlin "corner functions". These corner functions model the singular vibratory moments and shear forces, which simultaneously exist at the vertex of corner angle exceeding 180^0. The first set guarantees convergence to the exact frequencies as sufficient terms are taken. The second set represents the corner singularities, and accelerates convergence substantially. Numerical results are obtained for completely free sectorial plates. Accurate frequencies are presented for a wide spectrum of vertex angles (90^0, 180^0, 270^0, 300^0, 330^0, 350^0, 355^0, and 359^0) and thickness ratios.

1. INTRODUCTION

The problem of free vibration of complete circular and annular, thin and thick plates has attracted the attention of many researchers. However, the scope of previous work done for the sectorial plates (see Fig. 1) is narrow. Several researchers have offered theoretical and experimental vibration data for classically thin sectorial plates with various edge conditions on the circular and radial edges, namely on the work of Ben-Amoz[1], Bhattacharya and Bhowmic[2], Maruyama and Ichinomiya[3], Leissa *et al.*[4].

First order shear deformation theories by Reissner[5] and Mindlin[6], which include the effect of shear deformation and rotary inertia, have also been used in the vibration analysis of moderately thick annular sectorial plates. Bapu Rao *et al.*[7] developed various sector plate finite elements based on Reissner plate theory for approximate vibration analysis of thick circular and annular sectorial plates. Mizusawa[8] also proposed a Mindlin plate finite strip method for the vibration of thick annular plates having simply supported radial edges and arbitrary circular edge conditions. Srinivasan and Thiruvenkatachari[9] presented natural frequencies of annular sector Mindlin plates with all clamped edges by using the boundary element method. Recently, Huang *et al.*[10] provided exact analytical solutions for the free vibrations of Mindlin sectorial plates with simply supported radial edges that formed reentrant corners having unbounded bending stresses, and arbitrary circumferential edge conditions.

This paper provides a new comprehensive data base of accurate frequency solutions and mode shapes for completely free Mindlin sectorial plates. A Ritz procedure is employed which incorporates a complete set of admissible algebraic-trigonometric polynomials in conjunction with an admissible set of Mindlin corner functions. These corner functions model the singular vibratory moments and shear forces which simultaneously exist at the vertices of corner angles (α) exceeding 180^0. The first set guarantees convergence to exact frequencies when sufficient terms are retained. The second set substantially accelerates frequency convergence, which is demonstrated using numerical studies. Accurate frequencies are presented for a wide spectrum of vertex angles (α) (90^0, 180^0, 270^0, 300^0, 330^0, 350^0, 355^0, and 359^0) and thickness ratios (a/h).

2. METHODOLOGY

Consider in Fig. 1 a completely free, thick isotropic sectorial plate having radius a and thickness h with polar coordinates (r,θ) at the middle surface. The vibratory rotations and a transverse displacement are assumed in terms of polar coordinates (r,θ) at the middle surface as

*서울산업대학교 구조공학과, 시간강사
**정회원, 서울산업대학교 구조공학과, 부교수

$$\phi_r(r,\theta,t)=\Phi_r(r,\theta)\sin\omega t,\quad \phi_\theta(r,\theta,t)=\Phi_\theta(r,\theta)\sin\omega t,\quad w_z(r,\theta,t)=W_z(r,\theta)\sin\omega t, \tag{1}$$

where t is time and ω is the circular frequency of vibration.

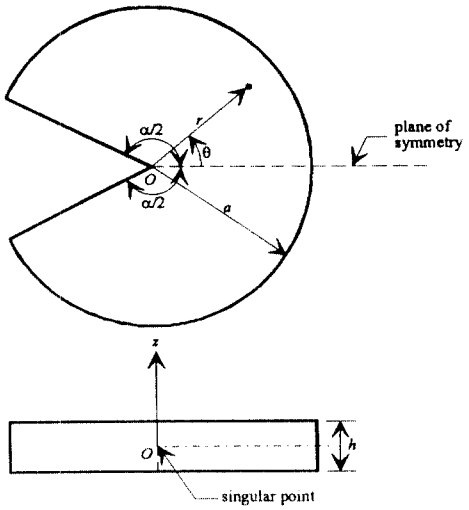

Fig.1 Geometry of thick sectorial plate

The maximum strain energy due to bending during a vibratory cycle is

$$V_{\max}=\frac{1}{2}\iint\left\{D\left[\left(\frac{\partial\Phi_r}{\partial r}\right)^2+\frac{1}{r^2}\left(\Phi_r+\frac{\partial\Phi_\theta}{\partial\theta}\right)^2+\frac{2\nu}{r}\frac{\partial\Phi_r}{\partial r}\left(\Phi_r+\frac{\partial\Phi_\theta}{\partial\theta}\right)\right.\right.$$
$$\left.\left.+\frac{(1-\nu)}{2}\left(\frac{1}{r}\frac{\partial\Phi_r}{\partial\theta}-\frac{\Phi_\theta}{r}+\frac{\partial\Phi_r}{\partial r}\right)^2\right]+\kappa^2Gh\left[\left(\Phi_r+\frac{\partial W_z}{\partial r}\right)^2+\left(\Phi_\theta+\frac{1}{r}\frac{\partial W_z}{\partial\theta}\right)^2\right]\right\}rdrd\theta, \tag{2}$$

where $D=Eh^3/12(1-\nu)$ is flexural rigidity, $G=E/2(1+\nu)$ is shear modulus, E is Young's modulus, ν is Poisson's ratio, and κ^2 is shear correction factor. The maximum kinetic energy is

$$T_{\max}=\frac{\rho\omega^2}{2}\iint\left[hW_z^2+\frac{h^3}{12}\left(\Phi_r^2+\Phi_\theta^2\right)\right]rdrd\theta, \tag{3}$$

in which ρ is the mass per unit area of the plate.

In the present Ritz approach, displacement trial functions are assumed as the sum of two finite sets:

$$\Phi_r=\Phi_r^p+\Phi_r^c,\quad \Phi_\theta=\Phi_\theta^p+\Phi_\theta^c,\quad W_z=W_z^p+W_z^c, \tag{4}$$

where Φ_r^p, Φ_θ^p, W_z^p are algebraic-trigonometric polynomials and Φ_r^c, Φ_θ^c, W_z^c are Mindlin corner functions. The admissible polynomials are written as

$$\Phi_r^p=\sum_{m=2,4}^{M_1}\sum_{n=0,2,4}^{m}A_{mn}r^{m-1}\cos n\theta+\sum_{m=1,3,5}^{M_2}\sum_{n=1,3,5}^{m}A_{mn}r^{m-1}\cos n\theta, \tag{5a}$$

$$\Phi_\theta^p = \sum_{m=2,4}^{M_3}\sum_{n=2,4}^{m} B_{mn} r^{m-1}\sin n\theta + \sum_{m=1,3,5}^{M_4}\sum_{n=1,3,5}^{m} A_{mn} r^{m-1}\sin n\theta, \tag{5b}$$

$$W_r^p = \sum_{m=0,2,4}^{M_5}\sum_{n=0,2,4}^{m} C_{mn} r^m \cos n\theta + \sum_{m=1,3,5}^{M_6}\sum_{n=1,3,5}^{m} C_{mn} r^m \cos n\theta, \tag{5c}$$

for the symmetric vibration modes, and

$$\Phi_r^p = \sum_{m=2,4}^{M_1}\sum_{n=2,4}^{m} D_{mn} r^{m-1}\sin n\theta + \sum_{m=1,3,5}^{M_2}\sum_{n=1,3,5}^{m} D_{mn} r^{m-1}\sin n\theta, \tag{6a}$$

$$\Phi_\theta^p = \sum_{m=2,4}^{M_3}\sum_{n=0,2,4}^{m} E_{mn} r^{m-1}\cos n\theta + \sum_{m=1,3,5}^{M_4}\sum_{n=1,3,5}^{m} E_{mn} r^{m-1}\cos n\theta, \tag{6b}$$

$$W_r^p = \sum_{m=2,4}^{M_5}\sum_{n=2,4}^{m} C_{mn} r^m \sin n\theta + \sum_{m=1,3,5}^{M_6}\sum_{n=1,3,5}^{m} C_{mn} r^m \sin n\theta, \tag{6c}$$

for the antisymmetric modes. In Eqs. (5) and(6), A_{mn}-F_{mn} are arbitrary coefficients, and the values of m and n have been specially chosen to eliminate those terms which yield undesirable singularities at $r = 0$ and yet preserve the mathematical completeness of the resulting series, as sufficient terms are retained. Thus, convergence to the exact frequencies is guaranteed when the series is employed in the present Ritz procedure.

The displacement polynomial Eqs. (5) and (6) should, in principle, yield accurate frequencies. However, the number of terms may be computationally prohibitive. This problem is alleviated by augmentation of the displacement polynomial trial set with admissible "corner functions", which introduce the proper singular vibratory shear forces and moments at the vertex of the V-notch (Fig. 1). The set of corner functions is taken as, for the symmetric modes:

$$\Phi_r^c = \sum_{k=1}^{K_1} G_k r^{\lambda_k}\left[\zeta_k \cos(\lambda_k + 1)\theta - \gamma_k \cos(\lambda_k - 1)\theta\right], \tag{7a}$$

$$\Phi_\theta^c = \sum_{k=1}^{K_2} G_k r^{\lambda_k}\left[-\zeta_k \sin(\lambda_k + 1)\theta + \gamma_k \sin(\lambda_k - 1)\theta\right], \tag{7b}$$

$$W_z^c = \sum_{k=1}^{K_3} H_k r^{\hat{\lambda}_k + 1}\cos(\hat{\lambda}_k + 1)\theta, \tag{7c}$$

with

$$\zeta_k = \frac{(\gamma_k + 1)(\lambda_k - 1)\sin(\lambda_k - 1)\alpha/2}{2\lambda_k \sin(\lambda_k - 1)\alpha/2}, \qquad \text{where} \qquad \gamma_k = \frac{\lambda_k(1+\nu) - 3 + \nu}{\lambda_k(1+\nu) + 3 - \nu}. \tag{7d}$$

In Eqs. (7), the λ_k and $\hat{\lambda}_k$ are the roots of the characteristic equations

$$\sin\lambda_k\alpha = -\lambda_k \sin\alpha, \qquad \sin(\hat{\lambda}_k + 1)\alpha/2 = 0. \tag{8}$$

Similarly, the corner functions used for antisymmetirc modes are analogous to those defined for the symmetric ones in Eqs. (7), except the cosine functions are changed to sine functions, or vice versa, and the corresponding characteristic equations are

$$\sin\lambda_k\alpha = \lambda_k \sin\alpha, \qquad \cos(\hat{\lambda}_k + 1)\alpha/2 = 0. \tag{9}$$

Some of the λ_k obtained from Eqs. (8) and (9) may be complex numbers, and thus result in complex corner functions. In such cases, both the real and imaginary parts are used as independent functions in the present Riz procedure.

The free vibration problem is solved by substituting Eqs. (4)-(7) into Eqs. (2) and (3) and employing the frequency equations of the Ritz method. For the symmetric modes, for example, these are:

$$\frac{\partial(V_{max}-T_{max})}{\partial A_{mn}}=0,\quad \frac{\partial(V_{max}-T_{max})}{\partial B_{mn}}=0,\quad \frac{\partial(V_{max}-T_{max})}{\partial C_{mn}}=0, \tag{10a}$$

$$\frac{\partial(V_{max}-T_{max})}{\partial G_k}=0,\quad \frac{\partial(V_{max}-T_{max})}{\partial H_k}=0. \tag{10b}$$

This results in a set of linear homogeneous algebraic equations involving the coefficients A_{mn}, B_{mn}, C_{mn}, G_k, and H_k. The vanishing determinant of these equations yields a set of eigenvalues (natural frequencies), expressed in terms of the non-dimensional frequency parameter, $\omega a^2(\rho/D)^{1/2}$ commonly used in the plate vibration literature. Eigenvectors involving the coefficients A_{mn}, B_{mn}, C_{mn}, G_k, and H_k are determined in the usual manner by substituting the eigenvalues back into the homogeneous equations. Normalized contours of the associated mode shapes are depicted on a r-θ grid in the circular plate domain, once the eigenvectors are substituted in Eqs. (4).

3. CONVERGENCE STUDIES

Having outlined the Ritz procedure employed in the preceding sections, it is now appropriate to address the important question of the convergence accuracy of frequencies as sufficient numbers of algebraic-trigonometric polynomials and Mindlin corner functions are retained. All of the frequency data discussed in the present section and following sections are for materials having shear correction factor κ^2 equal to $\pi^2/12$ and Poisson's ratio ν equal to 0.3. Numerical calculations of all frequencies were performed on an IBM/RS-6000 970 powerserver with an IBM workstation cluster using extended precision (28 significant figure) arithmetic.

Table 1 Convergence of frequency parameters $\omega a^2(\rho/D)^{1/2}$ for a completely free Mindlin sectorial plate ($\alpha = 355^0$, $a/h = 20$)

Mode no. (sym. Class*)	No. of Corner Functions	Solution size of polynomials				
		18	19	20	21	22
1 (A)	0	5.295	5.295	5.295	5.295	5.295
	1	5.158	5.153	5.147	5.141	5.136
	5	2.903	2.887	2.875	2.863	2.854
	10	2.870	2.860	2.852	2.844	2.838
	20	2.833	2.828	2.823	2.819	2.815
	30	2.823	2.819	2.815	2.811	2.808
	40	2.820	2.816	2.812	2.809	2.805
2 (S)	0	5.354	5.353	5.351	5.350	5.349
	1	5.081	5.059	5.042	5.020	5.005
	5	4.345	4.342	4.340	4.336	4.334
	10	4.323	4.322	4.321	4.319	4.318
	20	4.321	4.320	4.319	4.317	4.316
	30	4.321	4.319	4.318	4.317	4.316
	40	4.320	4.319	4.318	4.317	4.316
3 (S)	0	8.952	8.951	8.950	8.948	8.947
	1	8.489	8.457	8.436	8.405	8.384
	5	7.708	7.704	7.701	7.697	7.695
	10	7.680	7.679	7.678	7.676	7.676
	20	7.678	7.676	7.675	7.674	7.673
	30	7.677	7.676	7.675	7.674	7.673
	40	7.677	7.676	7.675	7.674	7.673

*(S)symmetric mode; (A)antisymmetric mode

Summarized in Table 1 is the first three non-dimensional frequency parameter $\omega a^2(\rho/D)^{1/2}$ for a completely free Mindlin sectorial plate with vertex angle (α) of 355^0 and with thickness ratio (a/h) of 20. This example is appropriately described as a Mindlin circular plate with a sharp notch or radial crack. Numerical results are shown as 19, 20, 21, and 22 polynomial solutions are retained in conjunction with 0, 1, 5, 10, 20, 30, and 40 Mindlin corner functions employed for each symmetry class. The solution size of the polynomials describes the number of upper

indices M_q, where q = 1, 2, 3, 4, 5, and 6 in the Eqs. (5) and (6). An equal number for M_q (i.e., $M_1 = M_2 = M_3 = M_4 = M_5 = M_6$) was used for each of the displacements. Similarly, an equal number of corner functions (i.e., ., $M_1 = M_2 = M_3$ in Eqs. (7)) was used for each of the rotations and transverse displacements. It should be noted that there are three rigid body modes in the vibration of the completely free Mindlin sectorial plate which are not shown in the table.

It can be seen in Table 1 that the fundamental (lowest) frequency mode is an antisymmetric one. An upper bound convergence of frequencies to an inaccurate value of 5.295 is apparent, as the sizes of polynomial series are increased with no Mindlin corner functions. One can see in Table 1 that adding a single corner function (corresponding to the lowest λ_k and $\hat{\lambda}_k$) impacts the convergence rate only slightly. However, adding five corner functions improves the convergence rate significantly. Indeed, the trial set consisting of the first five corner functions along with 18 polynomial solutions yields an upper bound frequency value of 2.903, which is much lower than the 5.158 value obtained using a single Mindlin corner function. An examination of the next four rows of data reveals that an accurate value to four significant figures is 2.805.

4. FREQUENCY RESULTS

In Table 2, extensive convergence studies were performed to compile the least upper bound frequency parameters $\omega a^2(\rho/D)^{1/2}$ for the first six modes of completely free Mindlin sectorial plates with various vertex angles (α = 90°, 180°, 270°, 300°, 330°, 350°, 355°, and 359°) and two different thickness ratios (i.e., a/h = 10 and 20). Frequency solutions previously reported by Irie, *et al.*[x] for Mindlin circular plate are also listed in Table 2. Frequency data corresponding to the antisymmetric modes are indicated by an asterisk (*). All frequncy results are guaranteed upper bounds to the exact values (accurate ti the four significant figures shown in Table 2). Hence, an accurate data base of frequencies for completely free Mindlin sectorial plates is presented in Table 2.

Table 2 Frequency parameters $\omega a^2(\rho/D)^{1/2}$ for completely free Mindlin sectorial plates

α	a/h	Mode Number					
		1	2	3	4	5	6
90°	20	15.86	22.79*	29.94	37.29*	55.63	64.77*
	10	15.38	22.00*	28.67	35.25*	51.66	59.57*
180°	20	6.893	9.355*	17.81*	17.90	28.56*	28.69
	10	6.813	9.145*	17.30*	17.37	27.35*	27.58
270°	20	4.556*	5.957	9.212	12.67*	17.01*	18.43
	10	4.455*	5.860	9.065	12.29*	16.40*	17.89
300°	20	3.766*	5.477	8.267	10.57*	15.40	16.53*
	10	3.675*	5.379	8.155	10.29*	15.01	15.80*
330°	20	3.179*	4.852	7.850	8.886*	13.02	16.04*
	10	3.100*	4.757	7.737	8.677*	12.73	15.27*
350°	20	2.869*	4.419	7.702	7.956*	11.74	15.17*
	10	2.794*	4.330	7.580	7.780*	11.50	14.54*
355°	20	2.805*	4.316	7.673	7.747*	11.46	14.88*
	10	2.729*	4.228	7.548	7.577*	11.23	14.29*
359°	20	2.760*	4.235	7.586*	7.651	11.24	14.64*
	10	2.680*	4.418	7.420*	7.523	11.02	14.08*
Circ**	20	5.330*	5.330	8.969	12.31*	12.31	20.26*
	10	5.278*	5.278	8.868	12.06*	12.06	19.71*

*Antisymmetric modes

**Results for complete circular plates given by Irie *et al.*[11]

From Table 2, it is seen that as the vertex angle α is increased, the frequencies are significantly decreased for any given a/h ratios. This reveals that for completely free sectorial plates the flexural stiffness decreases as the vertex angle increases. The frequency results listed in Table 2 for α = 359° may be described as for a completely free Mindlin circular plates having a sharp radial crack. It is important to compare the frequency data for plates with a sharp crack with the data for a compete circular plate. For the case of a/h = 20, the crack reduces the frequencies of

symmetric modes 2, 4, and 5 by 20.54%, 14.70%, and 8.69%, respectively, and those of the antisymmetric modes 1, 3, and 6 by 48.22%, 38.28%, and 27.74%, respectively. On the other hand, for the case of a/h = 10, the percent reductions in the frequencies of the symmetric modes 2, 4, and 5 are 21.41%, 15.17%, and 8.62%, respectively, and those in the antisymmetric modes 1, 3, and 6 are 49.22%, 38.47%, and 28.56%, respectively. One can see that the frequency reductions of all modes due to crack are slightly higher for thicker plates (a/h = 10) than for thinner ones (a/h = 20).

For all range of vertex angles, the influence of shear deformation and rotary inertial on the frequencies related to a/h ratios can be detected from Table 2. One can see that the frequency reducing effects of shear deformation and rotary inertia with decreasing a/h are, in general, more significant for the antisymmetric modes.

5. CONCLUDING REMARKS

Highly accurate frequencies and mode shapes for completely free sectorial plates have been obtained using a novel Ritz procedure in conjunction with Mindlin plate theory. In this approximate procedure, the assumed displacements of the plate constitutes a hybrid set of complete algebraic-trigonometric polynomials along with Mindlin corner functions that account for singular bending moments and shear forces at the vertex of acute corner angles. The efficacy of such corner functions has been substantiated by an convergence study of non-dimensional frequencies.

Detailed numerical tables have been presented, showing the variations of non-dimensional frequencies (accurate to four significant figures) with two geometric parameters; namely, vertex angle α and thickness ratio a/h. Some fundamental understanding of the effect of highly localized stresses on the sectorial plate dynamics can be obtained through careful examination of the frequency data offered herein. Most of all, the accurate vibration data presented here serves as benchmark values for comparison with data obtained using modern experimental and alternative theoretical approaches.

REFERENCES

1. Ben-Amoz, M., "Note on Deflections and Flexural Vibrations of Clamped Sectorial Plates," *ASME Journal of Applied Mechanics*, Vol. 26, pp. 136-137, 1959.
2. Bhattacharya, A. P. and Bhowmic, K. N., "Free Vibrations of a Sectorial Plate," *Journal of Sound and Vibration*, Vol. 41, pp. 503-505, 1975.
3. Maruyama, K. and Ichinomiya, O., "Experimental Investigation of Free Vibrations of Clamped Sector Plates," *Journal of Sound and Vibration*, Vol. 74, pp. 563-573, 1981.
4. Leissa, A.W., McGee, O. G., and Huang, C. S., "Vibrations of Sectorial Plates Having Corner Stress Singularities," *ASME Journal of Applied Mechanics*, Vol. 60, pp. 134-140, 1993.
5. Reissner, E., "The Effects of Transverse Shear Deformation on the Bending of Elastic Plates," *ASME Journal of Applied Mechanics*, Vol. 12, pp. 69-77, 1945.
6. Mindlin, R. D., "Influence of Rotatory Inertia and Shear on Flexural Motions of Isotropic, Elastic Plates," *ASME Journal of Applied Mechanics*, Vol. 18, pp. 31-38, 1951.
7. Bapu Rao, M. N., Guruswamy, P., and Sampath Kumaran, K. S., "Finite Element Analysis of Thick Annular and Sector Plates," *International Journal of Nuclear Engineering Design*, Vol. 41, pp. 247-255, 1977.
8. Mizusawa, T., "Vibration of Thick Annular Sector Plates Using Semi-Analytical Methods," *Journal of Sound and Vibration*, Vol. 150, pp. 245-259, 1991.
9. Srinivasan, R. S. and Thiruvenkatachari, V., "Free Vibration of Transverse Isotropic Annular Sector Mindlin Plates," *Journal of Sound and Vibration*, Vol. 101, pp. 193-201, 1985.
10. Huang, C. S., McGee, O. G., and Leissa, A. W., "Exact Analytical Solutions for Free Vibrations of Thick Sectorial Plates with Simply Supported Radial Edges," *International Journal of Solids and Structures*, Vol. 31, pp. 1609-1631, 1994.
11. Irie, T., Yamada, G., and Aomura, S., "Natural Frequencies of Mindlin Circular Plates," *ASME Journal of Applied Mechanics*, Vol. 47, pp. 134-140, 1993.